Chemical Science

ROYAL SOCIETY OF CHEMISTRY

EDGE ARTICLE

View Article Online
View Journal | View Issue

Cite this: *Chem. Sci.*, 2021, **12**, 15151

All publication charges for this article have been paid for by the Royal Society of Chemistry

Received 15th August 2021
Accepted 4th November 2021

DOI: 10.1039/d1sc04486a

rsc.li/chemical-science

A stable triplet diradical emitter†

Zhongtao Feng,‡[a] Yuanyuan Chong,‡[b] Shuxuan Tang,[a] Yong Fang,[a] Yue Zhao,[a] Jun Jiang *[b] and Xinping Wang *[a]

Molecules with luminescence have been extensively investigated, but the luminescence of a stable molecule with a triplet ground state has not been observed. Synthesis of boron-containing radicals has attracted lots of interest because of their unique electronic structures and potential applications in organic semiconductors. Though some boron-based diradicals have been reported, neutral boron-containing diradicals with triplet ground states are rare. Herein two borocyclic diradicals with different substituents (**3** and **4**) have been isolated. Their electronic structures were investigated by EPR and UV spectroscopy, and SQUID magnetometry, in conjunction with DFT calculations. Both experiment and calculation suggest that **3** is an open shell singlet diradical while **4** is a triplet ground state diradical with a large singlet–triplet gap (0.25 kcal mol^{-1}). Both diradicals show multi fluorescence peaks (**3**: 414, 431, and 470 nm; **4**: 420, 433, and 495 nm). **3** displays multiple redox steps and is a potential material towards the design of high-density memory devices. **4** represents the first example of a neutral triplet boron-containing diradical with a strong ferromagnetic interaction, and also is the first stable triplet diradical emitter.

Introduction

Molecules with luminescence have drawn much attention because of their applications in organic electronic devices and chemical sensors.[1] Luminescent radicals with a doublet or triplet ground state are able to provide high-efficiency electroluminescent devices for avoiding the quenching of the spin-forbidden transition from the excited triplet to the ground state in closed-shell molecules.[2] However, in contrast to doublet molecules, luminescent triplet molecules have gained little attention. The fluorescence from a trimethylenemethane triplet diradical in frozen solvent glasses was reported in 2007,[3] but the luminescence of a stable molecule with a triplet ground state has not been observed.

Diradicals, species with two unpaired electrons, not only have a pivotal role in understanding the nature of chemical bonding and spin–spin interaction, but also show great potential in the field of organic electronics because of their unique electronic and magnetic properties.[4] Synthesis and isolation of boron-containing radicals is one of the most important topics in radical chemistry because of their interesting structure and physical properties, and they exhibit potential applications as functional materials in organic semiconductors.[5] Though a number of main group element-containing diradicals have been reported, neutral boron-containing diradicals are scarce.[6] Bertrand *et al.* isolated the first crystalline boron-containing diradical (**A**, Fig. 1).[6a] Braunschweig *et al.* used cyclic (alkyl)(amino)carbenes (CAACs) as neutral donor units to stabilize neutral boron-based diradicals (**B–F**).[6b–f] Until now, no example of neutral triplet boron-containing diradicals with a rather strong ferromagnetic interaction has been reported.[7]

Bidentate heterocyclic ligands are effective in achieving neutral boron-containing monoradicals.[8] Yamashita *et al.*

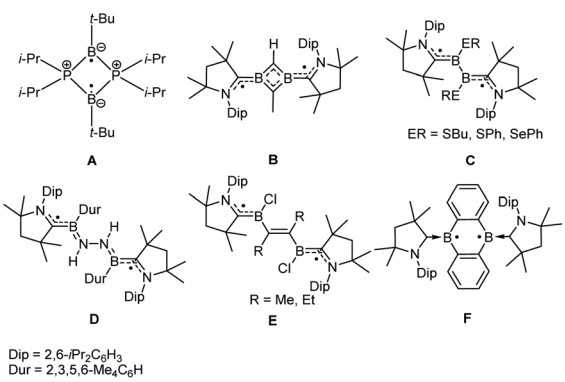

Fig. 1 Neutral structurally characterized boron-containing diradicals.

[a]*State Key Laboratory of Coordination Chemistry, School of Chemistry and Chemical Engineering, Collaborative Innovation Centre of Advanced Microstructures, Nanjing University, Nanjing 210023, China. E-mail: xpwang@nju.edu.cn*

[b]*Hefei National Laboratory for Physical Sciences at the Microscale, CAS Center for Excellence in Nanoscience, School of Chemistry and Materials Science, University of Science and Technology of China, Hefei, Anhui 230026, China. E-mail: jiangj1@ustc.edu.cn*

† Electronic supplementary information (ESI) available. CCDC 2079823 and 2079824. For ESI and crystallographic data in CIF or other electronic format see DOI: 10.1039/d1sc04486a

‡ These authors contributed equally to this work.

applied a β-diimine ligand to achieve a B-heterocyclic π-radical.[8c] Norman's group isolated a borocyclic radical with 4,4-dipyridyl.[8b] Fedushkin *et al.* obtained a diazaborocyclic radical through a redox-active diimine ligand.[8d] In the last few years, Stephan's group has synthesized a series of boron-containing radicals *via* frustrated Lewis pair hydrogenation reactions (4 atm, 110 °C).[8e,g,h,9] The first dithioborocyclic radical was reported by Robinson's group in 2018.[8i] Very recently, we achieved two dioxoborocyclic monoradicals with fluorescence in a high yield by a direct reduction reaction.[8k] On the other hand, recently Rajca and our group reported high-spin nitrogen-centered and sulfur–hydrogen diradical dications through pyrene or pyrene-like bridges.[10,11] Encouraged by these results, we speculate that neutral borocyclic diradicals with a triplet ground state and fluorescence through a pyrene bridge might be accessible. Herein, we report the synthesis and characterization of the borocyclic diradicals **3** and **4** using a direct method under mild conditions. The latter is the first stable triplet diradical emitter, and also the first neutral triplet boron-containing diradical with a rather strong ferromagnetic interaction (0.25 kcal mol^{-1}).

Results and discussion

Syntheses of 3 and 4

We first attempted to synthesize borocyclic diradicals **3** and **4** *via* similar frustrated Lewis pair hydrogenation reactions[8e,g,h,9] but failed due to the complexity of reaction. **3** and **4** were then synthesized in one step from corresponding tetraones (**1** and **2**) with chlorobis(perfluorophenyl)borane and potassium in THF (Fig. 2). They were isolated as red crystals in low yields and characterized by single-crystal X-ray diffraction, EPR and UV-vis spectroscopy, and SQUID magnetometry, together with theoretical calculations. Both compounds are air-sensitive, but can be stored in a glove box under a N_2 atmosphere at room temperature for several months.

Crystal structures

Crystals suitable for X-ray diffraction were obtained from the saturated toluene solutions of **3** and **4** at room temperature. Both of them crystallize in the triclinic space group $P\bar{1}$. The molecular structures of **3** and **4** are depicted in Fig. 3 and selected bond lengths and angles are given in Tables S2 and S3.† Crystallographic analysis of **3** and **4** reveals that both of them are centrosymmetric. The two BO2C2 rings are coplanar with

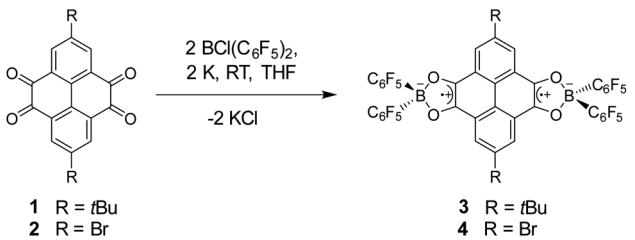

Fig. 2 Synthesis of diradicals **3** and **4**.

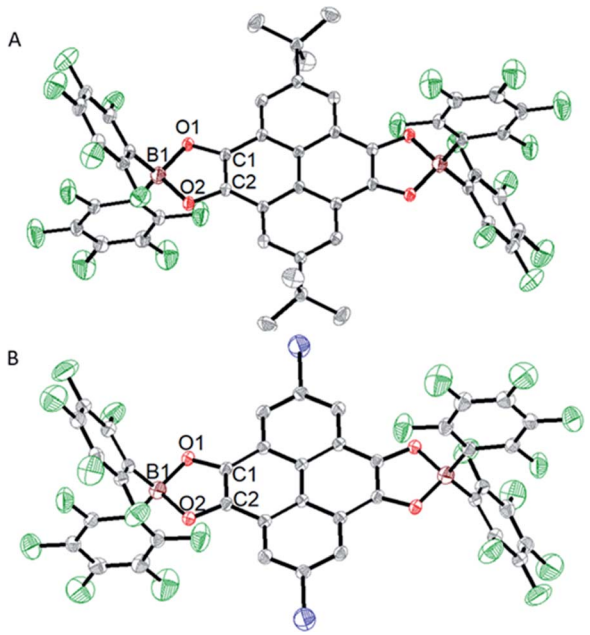

Fig. 3 Thermal ellipsoid drawings (at 50% probability) of **3** (A) and **4** (B). Hydrogen atoms and solvent molecules are omitted for clarity. Selected bond lengths (Å) and angles (°): **3** B1–O1 1.542(3), B1–O2 1.540(3), O1–C1 1.304(2), O2–C2 1.305(3), C1–C2 1.411(3), O1–B1–O2 100.81(16); **4** B1–O1 1.542(3), B1–O2 1.535(3), O1–C1 1.300(2), O2–C2 1.302(3), C1–C2 1.399(3), O1–B1–O2 100.90(16).

pyrenetetraone backbones. The average B–O distances (**3** 1.541 Å, **4** 1.538 Å) and O–B–O angles (**3** 100.81(16)°, **4** 100.90(16)°) of the two structures are similar, resembling those of the reported dioxoborocyclic monoradicals.[8g,k] The average C–O distances in **3** (1.304 Å) and **4** (1.301 Å) are longer than those in **1**[12] (1.214 Å) and **2** [13] (1.210 Å). Correspondingly, the average O–C–C angles (**3** 112°, **4** 112°) become more acute compared to those in **1** (118°) and **2** (119°). Notably, the C1–C2 bond length in **4** (1.399(3) Å) is slightly shorter than that in **3** (1.411(3) Å), but both are considerably shorter than those in the parent tetraones (**1** 1.546(1) Å, **2** 1.537(4) Å). The above changes from diradicals to neutral tetraones, together with other nearly unchanged bond parameters, indicate that unpaired electrons are mainly delocalized over the two BO2C2 rings. No obvious intermolecular interaction is observed in the crystal structures of **3** and **4**, which can be attributed to the two $-B(C_6F_5)_2$ steric-crowding substituent groups.

Magnetic studies

The magnetic properties of **3** and **4** were determined by EPR spectroscopy and SQUID magnetometry. The forbidden $\Delta m_s = \pm 2$ transitions were observed in the half regions of their EPR spectra (Fig. 4A and B), indicating that both of them are diradicals. The zero-field splitting (ZFS) parameters of crystalline **3** were determined by spectral simulation (D = 120 G, E = 25 G) with an anisotropic g factor ($g_x = g_y = 2.0042$, $g_z = 2.0011$). ZFS of **4** was not observed in the solid state (Fig. S1†) but observed in dibutyl phthalate (DBP) solution at 90 K with D = 118 G, E = 40 G and an anisotropic g factor ($g_x = g_y = 2.0047$, $g_z = 2.0060$). The g_{iso} factors

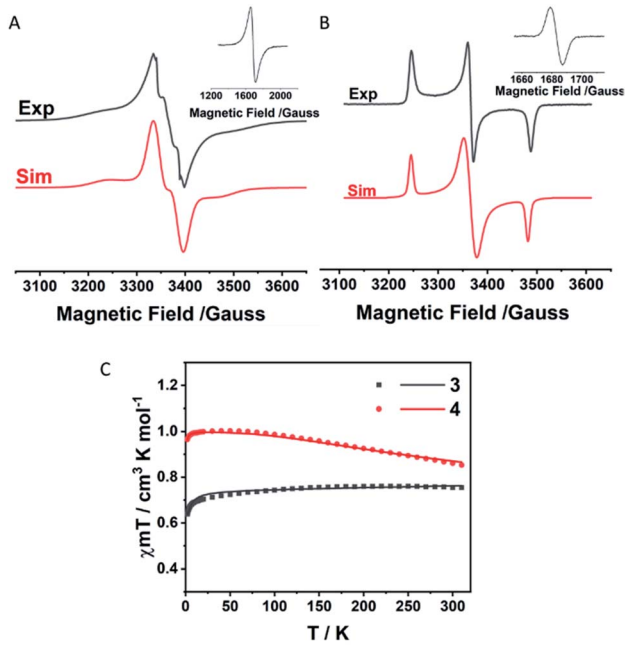

Fig. 4 EPR spectra and temperature-dependent plots of $\chi_M T$ of **3** and **4**. (A) The EPR spectrum of the powder sample of **3** at 90 K with the forbidden transition in the half magnetic field. (B) Frozen-solution EPR spectrum of 1×10^{-4} M **4** in dibutyl phthalate at 90 K with the forbidden transition in the half magnetic field. (C) $\chi_M T$ *versus* T curves (dot) in the SQUID measurements of the powder of **3** and **4**, and the fitting plots (line) obtained with the Bleaney–Bowers equation.[14]

(2.0032 for **3** and 2.0051 for **4**) are comparable to those of dioxoborocyclic monoradicals.[8g,k] The average spin–spin distances from D were estimated to be 6.14 Å for **3** and 6.18 Å for **4**, respectively, which are close to the distances between the two centers of BO2C2 rings in each (6.66 Å for **3** and 6.67 Å for **4**).

SQUID measurements on powder samples of **3** and **4** were carried out to determine their ground states. $\chi_M T$ of **3** (Fig. 4C) maintains 0.75 cm^3 $kmol^{-1}$ from 310 to 25 K and shows a decreasing susceptibility below 25 K, suggesting that **3** has a singlet open-shell ground state. In contrast, the increase of the susceptibility of **4** (Fig. 4C) from 310 (0.85 cm^3 $kmol^{-1}$) to 5 K (1.0 cm^3 $kmol^{-1}$) indicates that **4** has a triplet ground state. The

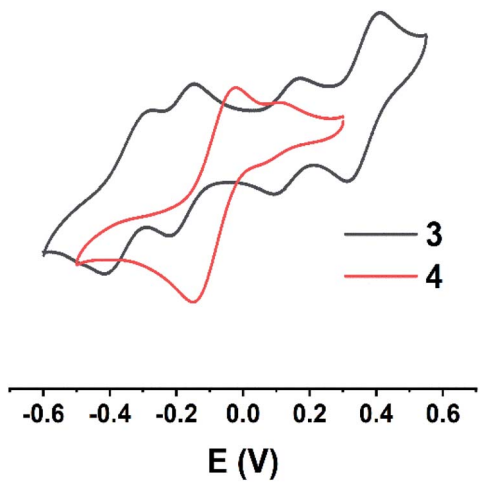

Fig. 5 Cyclic voltammograms of **3** and **4**.

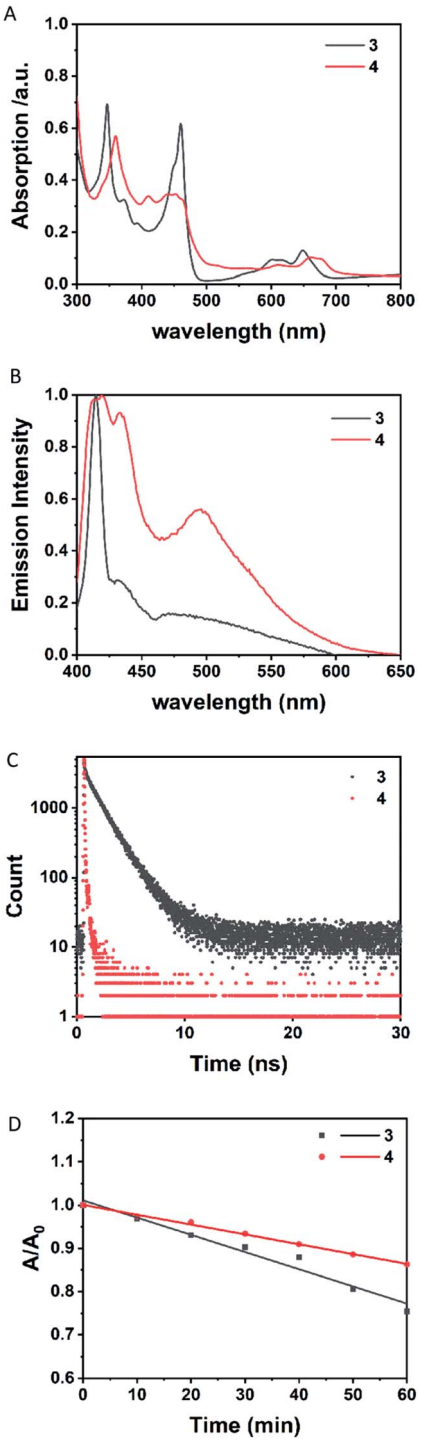

Fig. 6 (A) UV/vis absorption spectra of **3** and **4** in THF at room temperature. (B) Fluorescence spectra upon excitation at 370 nm of **3** and 375 nm of **4** in THF at room temperature. (C) Fluorescence decay of **3** and **4** following excitation at 375 nm. (D) Photo-stability analysis of **3** and **4** under irradiation (365 nm) for different times. A/A_0 represents the ratio of absorbance before and after irradiation for the corresponding time.

experimental data were fitted with the Bleaney–Bowers equation[14] with Hamiltonian $H = -2JS_1S_2$ ($S_1 = S_2 = 1/2$), giving the singlet–triplet energy gaps $\Delta E_{OS-T} = 2J = -1.24$ cal mol^{-1} for **3** and 251.6 cal mol^{-1} for **4**, respectively. The different ground states of **3** and **4** are associated with the electronic effect of the substituent groups at the 2 and 7 positions of the pyrenetetraone backbone.

Electrochemical properties

The cyclic voltammogram of **3** in THF (Fig. 5) shows two reversible reduction waves at −0.19 and −0.36 V and two reversible oxidation waves at 0.12 and 0.35 V *vs.* Ag/AgNO$_3$, while that of **4** (Fig. 5) only shows one reversible reduction wave at −0.09 V and one irreversible oxidation wave at 0.08 V, indicating remarkable substituent dependence. The cyclic voltammogram of **3** suggests that it can be reversibly reduced and oxidized to the corresponding radical anion, dianion, radical cation and dication under the CV conditions. Diradical **3** with multiple redox steps is a potential material for the design of high-density memory devices compared with the reported perchlorotriphenylmethyl (PTM) radical (one reversible reduction wave at −0.3 V).[4g,15]

Optical properties

The UV-vis spectrum of **3** (Fig. 6A) in dilute THF shows two strong absorptions at 347 and 461 nm and two weak absorptions at 618 and 649 nm. Similarly, the UV-vis spectrum of **4** (Fig. 6A) shows two strong absorptions at 359 and 454 nm and two weak absorptions at 612 and 663 nm. The fluorescence spectrum of **3** (Fig. 6B) in THF upon excitation at $\lambda_{exc} = 370$ nm shows a maximum emission at 414 nm with two weak bands at 431 and 470 nm. The fluorescence spectra of **4** (Fig. 6B) show a maximum emission at 420 nm with two bands at 433 and 495 nm. The diradicals **3** and **4** do not obey Kasha's rule, as found previously for borocyclic monoradical emitters.[8k] The fluorescence emissions of **3** and **4** arise from the return from higher excited states to the ground state. The photoluminescence quantum yields (PLQY) of **3** and **4** were measured to be 0.15%, 0.30%, and the lifetimes of **3** and **4** were 15.9 and 0.11 ns, respectively. The photostabilities (Fig. 6D) of **3** (125 min) and **4** (219 min), which were represented by half-life ($t_{1/2}$), were obtained from the fitting plot of A/A_0–t.

Theoretical calculations

To have a better understanding of the electronic structures of diradicals **3** and **4**, DFT calculations were performed using the Gaussian16 program at the (U)B3LYP/6-31G(d) level of theory.[16] **3** is stable as a singlet in the ground state (ΔE_{OS-T} = 0.022 kcal mol^{-1}) while **4** has a triplet ground state (ΔE_{OS-T} = −0.718 kcal mol^{-1}), consistent with the experimental result. The spin densities in **3** and **4** indicate that the substituents affect the extent of diradical delocalization to control the ground states. Two *t*Bu groups in **3** show an electron donating

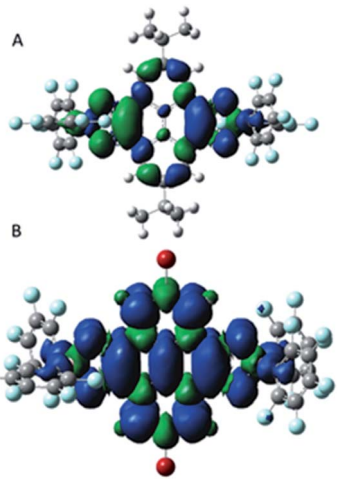

Fig. 7 Spin densities of **3** (A) and **4** (B) calculated at the UB3LYP/6-31G(d) level.

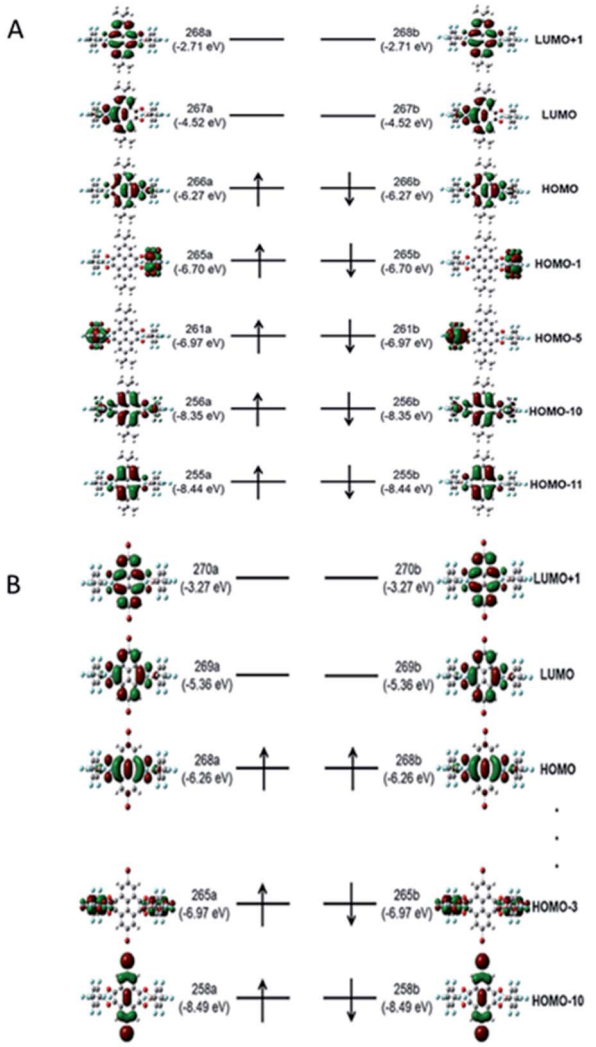

Fig. 8 (A) Ground state frontier (and adjacent) molecular orbitals of diradical **3** from the unrestricted Kohn–Sham (UKS) DFT calculation (UB3LYP, 6-31g(d), in a vacuum). (B) Ground state frontier (and adjacent) molecular orbitals of diradical **4** from the unrestricted Kohn–Sham (UKS) DFT calculation (UB3LYP, 6-31g(d), in a vacuum).

inductive effect (+I) and the spin densities in **3** are mainly distributed among the two BO2CO rings (Fig. 7A). In sharp contrast, the spins in **4** are distributed throughout the whole pyrenetetraone backbones (Fig. 7B), which is attributed to the electron withdrawing inductive effect (−I) of the two Br groups.[17] Substituents with different polarities lead to a change in the charge recombination free energy (ΔG) while the solvent reorganization energy (λ) remains constant. Those will affect the sign of the electron exchange interaction (J) value. Meanwhile, the J value is defined by the energy separation between singlet and triplet radical pairs ($2J = E_{OS} - E_T$). Therefore, substituents with different inductive effect (+I or −I) effect on singlet-triplet energy ordering to determine which the ground state is by influencing the J value.[18]

Likewise, the molecular photophysical properties of diradicals **3** and **4** can be explored by unrestricted Kohn–Sham DFT (UKS-DFT)[19] and time dependent DFT (TDDFT)[20] calculations with the (U)B3LYP functional and 6-31g(d) basis set. The strong absorption peaks appearing in the experiment have a good agreement with theoretical calculations for both **3** and **4** (Tables S6 and S7,† sample in a vacuum). Thus, the orbital transition nature of the excited states corresponding to the absorption peak is revealed (Fig. 8A and B). The two strong absorption peaks in **3** are both attributed to alpha (spin-up) and beta (spin-down) electron transitions from their respective (HOMO−n) to LUMO orbitals (Table S6†). The (HOMO−3) → (LUMO+1) transition contributes to a strong absorption peak on the left side (experimental, 359 nm; theoretical, 378 nm) in **4**, while that on the right side (experimental, 454 nm; theoretical, 474 nm) is also ascribed to the (HOMO−n) → LUMO orbital transition (Table S7†).

Conclusions

We have synthesized two borocyclic diradicals **3** and **4** in one step under mild conditions, and they were characterized by single crystal X-ray diffraction, EPR and UV-vis spectroscopy, and SQUID magnetometry. Both experiment and calculation suggest that **3** is an open shell singlet diradical while **4** is a triplet ground state diradical. The experimental and theoretical studies of **3** and **4** reveal that the ground states of diradicals could be adjusted by the inductive effect of substituent groups. **4** also represents a rare example of neutral triplet boron-containing diradicals with strong ferromagnetic coupling and the first stable triplet diradical emitter. Diradicals with multiple redox are scarce and **3** is a potential material towards the design of high-density memory devices compared with the PTM radicals.[4g,15] In addition, such borocyclic diradicals are easier to modify with other substituents and show multi functionalization. Further work about the photoluminescence mechanism of diradicals and other functional investigations on these newly formed diradicals is continuous in our laboratory.

Data availability

Crystallographic data for **3** and **4** have been deposited in the Cambridge Crystallographic Data Center under CCDC no. 2079823 and 2079824.

Author contributions

X. W. conceived the project. Z. F. did the experiments and data analysis and participated in the writing. X. W. wrote the manuscript. Y.C. carried out the calculations. J. J. analyzed the computational data and wrote the theoretical part. S. T. performed the SQUID measurement. Y. F. performed the EPR measurement. Y. Z. performed the X-ray diffraction studies. All authors discussed the results and manuscript.

Conflicts of interest

There are no conflicts to declare.

Acknowledgements

We thank the National Key R&D Program of China (Grants 2016YFA0300404 and 2018YFA0306004 X. W.), the National Natural Science Foundation of China (Grants 21525102 and 21690062 X. W.; 22033007 and 22025304 J. J.) and CAS Project for Young Scientists in Basic Research (Grant YSBR-005 J. J.) for financial support. The calculations were performed at the High-Performance Computing Center of Nanjing University and the Supercomputing Center of University of Science and Technology of China.

Notes and references

1 (*a*) C. W. Tang and S. A. VanSlyke, *Appl. Phys. Lett.*, 1987, **51**, 913–915; (*b*) X. H. Zhu, J. Peng, Y. Cao and J. Roncali, *Chem. Soc. Rev.*, 2011, **40**, 3509–3524; (*c*) H. Xu, R. Chen, Q. Sun, W. Lai, Q. Su, W. Huang and X. Liu, *Chem. Soc. Rev.*, 2014, **43**, 3259–3302; (*d*) R. Xu, Y. Li and J. Tang, *J. Mater. Chem. C*, 2016, **4**, 9116–9142.

2 (*a*) Z. Cui, A. Abdurahman, X. Ai and F. Li, *CCS Chem.*, 2020, **2**, 1129–1145; (*b*) X. Ai, E. W. Evans, S. Dong, A. J. Gillett, H. Guo, Y. Chen, T. Hele, R. Friend and F. Li, *Nature*, 2018, **563**, 536–540; (*c*) A. Abdurahman, T. Hele, Q. Gu, J. Zhang, Q. Peng, M. Zhang, R. Friend, F. Li and E. Evans, *Nat. Mater.*, 2020, **19**, 1224–1229; (*d*) Q. Peng, A. Obolda, M. Zhang and F. Li, *Angew. Chem., Int. Ed.*, 2015, **127**, 7197–7201; (*e*) Y. Hattori, T. Kusamoto and H. Nishihara, *Angew. Chem., Int. Ed.*, 2014, **44**, 11845–11848; (*f*) Y. Hattori, T. Kusamoto and H. Nishihara, *Angew. Chem., Int. Ed.*, 2015, **54**, 3731–3734; (*g*) C. Liu, E. Hamzehpoor, Y. S. Otsuka, T. Jadhav and D. Perepichka, *Angew. Chem. Int. Ed.*, 2020, **59**, 23030–23034.

3 N. Hayato, I. Hiroshi, H. Yosuke, K. Nobuyuki, M. Yoshii and M. Kazuhiko, *J. Am. Chem. Soc.*, 2007, **129**, 9032–9036.

4 (*a*) L. Salem and C. Rowland, *Angew. Chem., Int. Ed. Engl.*, 1972, **11**, 92–111; (*b*) F. Breher, *Coord. Chem. Rev.*, 2007, **251**, 1007–1043; (*c*) M. Abe, J. Ye and M. Mishima, *Chem. Soc. Rev.*, 2012, **41**, 3808–3820; (*d*) Z. Sun, Q. Ye, C. Chi and J. Wu, *Chem. Soc. Rev.*, 2012, **41**, 7857–7889; (*e*) M. Abe, *Chem. Rev.*, 2013, **113**, 7011–7088; (*f*) Z. Zeng, X. Shi, C. Chi, J. T. López Navarrete, J. Casado and J. Wu, *Chem. Soc. Rev.*, 2015, **44**, 6578–6596; (*g*) X. Hu, W. Wang,

D. Wang and Y. Zheng, *J. Mater. Chem. C*, 2018, **6**, 11232–11242; (*h*) T. Stuyver, B. Chen, T. Zeng, P. Geerlings, F. De Proft and R. Hoffmann, *Chem. Rev.*, 2019, **119**, 11291–11351.

5 (*a*) P. P. Power, *Chem. Rev.*, 2003, **103**, 789–810; (*b*) W. Kaim, N. S. Hosmane, S. Záliš, J. A. Maguire and W. N. Lipscomb, *Angew. Chem., Int. Ed.*, 2009, **48**, 5082–5091; (*c*) R. Hicks, *Stable radicals*. John Wiley & Sons, Ltd, 2010; (*d*) P. Renaud, *Boron in radical chemistry*. John Wiley & Sons, Ltd, 2012; (*e*) T. Chivers and J. Konu, *Comprehensive Inorganic Chemistry II*, Elsevier, 2nd edn, 2013, 1, pp. 349–373; (*f*) Y. Su and R. Kinjo, *Coord. Chem. Rev.*, 2017, **352**, 346–378.

6 (*a*) D. Scheschkewitz, H. Amii, H. Gornitzka, W. W. Schoeller, D. Bourissou and G. Bertrand, *Science*, 2002, **295**, 1880–1881; (*b*) M. Arrowsmith, J. Böhnke, H. Braunschweig, M. A. Celik, C. Claes, W. C. Ewing, I. Krummenacher, K. Lubitz and C. Schneider, *Angew. Chem., Int. Ed.*, 2016, **55**, 11271–11275; (*c*) J. Böhnke, T. Dellermann, M. A. Celik, I. Krummenacher, R. D. Dewhurst, S. Demeshko, W. C. Ewing, K. Hammond, M. Heß, E. Bill, E. Welz, M. I. S. Röhr, R. Mitrić, B. Engels, F. Meyer and H. Braunschweig, *Nat. Commun.*, 2018, **9**, 1197–1203; (*d*) M. A. Legare, G. Belanger-Chabot, R. D. Dewhurst, E. Welz, I. Krummenacher, B. Engels and H. Braunschweig, *Science*, 2018, **359**, 896–900; (*e*) A. Deissenberger, E. Welz, R. Drescher, I. Krummenacher, R. D. Dewhurst, B. Engels and H. Braunschweig, *Angew. Chem., Int. Ed.*, 2019, **58**, 1842–1846; (*f*) C. Saalfrank, F. Fantuzzi, T. Kupfer, B. Ritschel, K. Hammond, I. Krummenacher, R. Bertermann, R. Wirthensohn, M. Finze, P. Schmid, V. Engel, B. Engels and H. Braunschweig, *Angew. Chem., Int. Ed.*, 2020, **59**, 19338–19343.

7 In 2017, we synthesized a triplet boron-containing diradical dianion with a very small singlet–triplet gap (0.0051 kcal mol^{-1}), L. Wang, Y. Fang, H. Mao, Y. Qu, J. Zuo, Z. Zhang, G. Tan and X. Wang, *Chem.–Eur. J.*, 2017, **23**, 6930–6936.

8 (*a*) A. Hinchliffe, F. S. Mair, E. J. L. McInnes, R. G. Pritchard and J. E. Warren, *Dalton Trans.*, 2008, 222–233; (*b*) S. M. Mansell, C. J. Adams, G. Bramham, M. F. Haddow, W. Kaim, N. C. Norman, J. E. McGrady, C. A. Russell and S. J. Udeen, *Chem. Commun.*, 2010, 5070–5072; (*c*) Y. Aramaki, H. Omiya, M. Yamashita, K. Nakabayashi, S. Ohkoshi and K. Nozaki, *J. Am. Chem. Soc.*, 2012, **134**, 19989–19992; (*d*) I. L. Fedushkin, O. V. Markina, A. N. Lukoyanov, A. G. Morozov, E. V. Baranov, M. O. Maslov and S. Y. Ketkov, *Dalton Trans.*, 2013, 7952–7961; (*e*) K. L. Bamford, L. E. Longobardi, L. Liu, S. Grimme and D. W. Stephan, *Dalton Trans.*, 2017, 5308–5319; (*f*) S. K. Pal, M. E. Itkis, F. S. Tham, R. W. Reed and R. T. Oakley, *Science*, 2005, **309**, 281–284; (*g*) L. E. Longobardi, L. Liu, S. Grimme and D. W. Stephan, *J. Am. Chem. Soc.*, 2016, **138**, 2500–2503; (*h*) L. E. Longobardi, P. Zatsepin, R. Korol, L. Liu, S. Grimme and D. W. Stephan, *J. Am. Chem. Soc.*, 2017, **139**, 426–435; (*i*) G. H. Robinson, Y. Wang, Y. Xie, P. Wei, S. Blair, D. Cui, M. K. Johnson and H. F. Schaefer, *Angew. Chem., Int. Ed.*, 2018, **57**, 7865–7868; (*j*) T. K. Wood, W. E. Piers, B. A. Keay and M. Parvez, *Chem. Commun.*, 2009, 5147–5149; (*k*) Z. Feng, C. Yuan, S. Tang, H. Ruan, Y. Fang, Y. Zhao, J. Jiang and X. Wang, *Chin. J. Chem.*, 2021, **39**, 1297–1302.

9 L. L. Liu and D. W. Stephan, *Chem. Soc. Rev.*, 2019, **48**, 3454–3463.

10 S. Tang, L. Zhang, H. Ruan, Y. Zhao and X. Wang, *J. Am. Chem. Soc.*, 2020, **142**, 7340–7344.

11 C. Shu, H. Zhang, A. Olankitwanit, S. Rajca and A. Rajca, *J. Am. Chem. Soc.*, 2019, **141**, 17287–17294.

12 Z. Wang, V. Enkelmann, F. Negri and K. Müllen, *Angew. Chem., Int. Ed.*, 2004, **43**, 1972–1975.

13 S. Kawano, M. Baumgarten, D. Chercka, V. Enkelmann and K. Müllen, *Chem. Commun.*, 2013, **49**, 5058–5060.

14 B. Bleaney, *Proc. R. Soc. London, Ser. A*, 1953, **25**, 161–162.

15 C. Simão, M. Mas-Torrent, N. Crivillers, V. Lloveras, J. M. Artes, P. Gorostiza, J. Veciana and C. A. Rovira, *Nat. Chem.*, 2010, **3**, 359–364.

16 M. J. Frisch, G. W. Trucks, H. B. Schlegel, G. E. Scuseria, M. A. Robb, J. R. Cheeseman, G. Scalmani, V. Barone, G. A. Petersson, H. Nakatsuji, X. Li, M. Caricato, A. V. Marenich, J. Bloino, B. G. Janesko, R. Gomperts, B. Mennucci, H. P. Hratchian, J. V. Ortiz, A. F. Izmaylov, J. L. Sonnenberg, D. Williams, F. Ding, F. Lipparini, F. Egidi, J. Goings, B. Peng, A. Petrone, T. Henderson, D. Ranasinghe, V. G. Zakrzewski, J. Gao, N. Rega, G. Zheng, W. Liang, M. Hada, M. Ehara, K. Toyota, R. Fukuda, J. Hasegawa, M. Ishida, T. Nakajima, Y. Honda, O. Kitao, H. Nakai, T. Vreven, K. Throssell, J. A. Montgomery Jr, J. E. Peralta, F. Ogliaro, M. J. Bearpark, J. J. Heyd, E. N. Brothers, K. N. Kudin, V. N. Staroverov, T. A. Keith, R. Kobayashi, J. Normand, K. Raghavachari, A. P. Rendell, J. C. Burant, S. S. Iyengar, J. Tomasi, M. Cossi, J. M. Millam, M. Klene, C. Adamo, R. Cammi, J. W. Ochterski, R. L. Martin, K. Morokuma, O. Farkas, J. B. Foresman and D. J. Fox, *Gaussian 16 Rev. C.01*, Wallingford, CT, 2016.

17 S. Tero-Kubota, K. Zikihara, T. Yago, Y. Kobori and K. Akiyama, *Appl. Magn. Reson.*, 2004, **26**, 145–154.

18 P. D. Silva, *J. Phys. Chem. Lett.*, 2019, **10**, 5674–5679.

19 J. A. Pople, P. M. Gill and N. C. Handy, *Int. J. Quantum Chem.*, 1995, **56**, 303–305.

20 A. D. Laurent and D. Jacquemin, *Int. J. Quantum Chem.*, 2013, **113**, 2019–2039.